Analysis of Open-Loop Conical Scan Pointing Error and Variance Estimators

L. S. Alvarez
Ground Antennas and Facilities Engineering Section

General pointing error and variance estimators for an open-loop conical scan (conscan) system are derived and analyzed. The conscan algorithm is modeled as a weighted least-squares estimator whose inputs are samples of receiver carrier power and its associated measurement uncertainty. When the assumptions of constant measurement noise and zero pointing error estimation are applied, the variance equation is then strictly a function of the carrier power-to-uncertainty ratio and the operator-selectable radius and period input to the algorithm. The performance equation is applied to a 34-m mirror-based beam-waveguide conscan system interfaced with the Block V Receiver Subsystem tracking a Ka-band (32-GHz) downlink. It is shown that for a carrier-to-noise power ratio ≥ 30 dB-Hz, *the conscan period for Ka-band operation may be chosen well below the current DSN minimum of* 32 *sec. The analysis presented forms the basis of future conscan work in both research and development as well as for the upcoming DSN antenna controller upgrade for the new DSS-24 34-m beam-waveguide antenna.*

I. Introduction

An analysis of open-loop conical scan (conscan) pointing error and variance estimators is presented. The analysis models conscan as a beam-pointing error sensor whose input consists of samples of receiver carrier power and uncertainty. This choice of input is consistent with the upcoming DSN upgrade of conscan that will involve the interfacing of the Antenna Pointing Controller and the Block V Receiver Subsystem. With this input, the conscan algorithm is modeled as a weighted least-squares estimator whose variance can be derived as a function of the uncertainty on the receiver input and the operator-selectable inputs to the algorithm. A general variance equation that is applicable to either conscan axis is derived and then simplified when assumptions of constant measurement uncertainty and zero pointing error are applied.

Estimation of the uncertainty on the carrier power samples from the Block V Receiver Subsystem is briefly reviewed, and the results are used to rewrite the conscan pointing-error-variance equation in terms of the carrier-to-noise power ratio. The final equation can then be used to easily quantify the pointing error uncertainty as a function of conscan radius and period for any given antenna's half-power beamwidth and receiver carrier-to-noise power operating condition. The article concludes with an application of the performance equation to a beam-waveguide mirror conscan implementation operating at the Ka-band (32-GHz) frequency.

II. Received Carrier Power Model For Conscan

The conical scan received signal model presented below is similar to the one described in [1]. The input to the conscan algorithm in this analysis will be estimates of received carrier power P_c with measurement uncertainty σ_{P_c}. The assumption here is that the digital receiver subsystem has derived both of these quantities from its estimate of signal-to-noise ratio P_c/N_o. The main results of this analysis will be general with respect to the conscan algorithm input and can be modified slightly to accommodate other received signal level input (e.g., voltages or noise temperatures).

The ratio of the received carrier power $P_{(t)}$ at time t to nominal carrier power P_{cnom} when the antenna boresight is pointing at the target is

$$\frac{P_c(t)}{P_{cnom}} = \exp\left(-\frac{\mu}{h^2}\varepsilon(t)^2\right) \quad (1)$$

where h is the antenna half-power beamwidth, $\mu = 4\ln(2)$, and $\varepsilon(t)$ is the angular displacement of the target to the center of the beam. During conscan, $\varepsilon(t)^2$ in [1] is shown to be

$$\varepsilon(t)^2 = r^2 + \varepsilon_s^2 - 2r\varepsilon_{xel}\cos(wt) - 2r\varepsilon_{el}\sin(wt) \quad (2)$$

where r is the conscan radius, w is the conscan frequency, and ε_{xel} and ε_{el} are cross-elevation and elevation components of the beam pointing error ε_s, defined as

$$\varepsilon_s^2 = \varepsilon_{xel}^2 + \varepsilon_{el}^2 \quad (3)$$

Let $L_1 = \exp\left((-\mu/h^2)r^2\right)$ be the loss factor when the target is at the center of the scan pattern and $L_2 = \exp\left((-\mu/h^2)\varepsilon_s^2\right)$ be the loss factor due to the beam-pointing error being estimated; then inserting Eq. (2) into Eq. (1) and simplifying yields

$$P_c(t) = P_{cnom}L_1L_2$$

$$\times \exp\left(\frac{2r\mu}{h^2}\left[\varepsilon_{xel}\cos(wt) + \varepsilon_{el}\sin(wt)\right]\right) \quad (4)$$

It can be shown that

$$P_o = P_{cnom}L_1L_2 \quad (5)$$

and

$$k_s = \frac{2r\mu}{h} \quad (6)$$

where P_o is the average carrier power received over the conical scan period and k_s is the conscan slope. Now for small target errors, the approximation $\exp(x) \approx 1 + x$ can be applied to Eq. (4), and then inserting Eqs. (5) and (6) gives the following:

$$P_c(t) = P_o\left(1 + \frac{k_s}{h}\varepsilon_{xel}\cos(wt) + \frac{k_s}{h}\varepsilon_{el}\sin(wt)\right) \quad (7)$$

or rewriting in vector notation,

$$P_c(t) = \begin{bmatrix} 1 & \cos(wt) & \sin(wt) \end{bmatrix} \begin{bmatrix} C_1 \\ C_2 \\ C_3 \end{bmatrix} \quad (8)$$

where $C_1 = P_o$, $C_2 = ((k_s/h)\varepsilon_{xel})P_o$, and $C_3 = ((k_s/h)\varepsilon_{xel})P_o$. Equation (8) is the measurement equation used along with P_c and σ_{P_c} in the conscan pointing error estimator.

III. General Pointing Error and Variance Estimators

A. Pointing Error Estimator

The conscan estimation period can be any interval of time and, in general, does not have to be a complete period of the sinusoid in Eq. (8); nor does receiver power have to be measured uniformly over this interval. However, the present analysis will assume received signal power $P_c(t)$ is uniformly sampled n times over a conscan period of T sec with a receiver integration time of t_{rec} sec, where $T = nt_{rec}$. Substituting $t = it_{rec}$ and $w = 2\pi/nt_{rec}$ in Eq. (8) yields the conscan carrier power measurement equation at the sampling instants i as

$$P_c(i) = \left[1 \quad \cos\left(\frac{2\pi}{n}i\right) \quad \sin\left(\frac{2\pi}{n}i\right)\right] \begin{bmatrix} C_1 \\ C_2 \\ C_3 \end{bmatrix} \quad (9)$$

Accumulating n input samples and storing them in matrix form gives

$$\begin{bmatrix} P_c(1) \\ P_c(2) \\ \vdots \\ P_c(n) \end{bmatrix} = \begin{bmatrix} 1 & \cos(\frac{2\pi}{n}) & \sin(\frac{2\pi}{n}) \\ 1 & \cos(2\frac{2\pi}{n}) & \sin(2\frac{2\pi}{n}) \\ & \vdots & \\ 1 & \cos(2\pi) & \sin(2\pi) \end{bmatrix} \begin{bmatrix} C_1 \\ C_2 \\ C_3 \end{bmatrix} \quad (10)$$

or

$$\mathbf{Y} = \mathbf{AC} \quad (11)$$

where the measurement vector $\mathbf{Y}$ is $n \times 1$, the measurement distribution matrix $\mathbf{A}$ is $n \times 3$, and the parameter vector $\mathbf{C}$ is 3×1. It is assumed that the uncertainties on the carrier power estimates at the sampling times, denoted as $\sigma_{P_c}(i)$, are also known and available. Assuming that the uncertainties are random and independent over the period T, they are accumulated in a weighting matrix $\mathbf{R}$ as follows:

$$\mathbf{R} = \text{diag}\left(\frac{1}{\sigma^2_{P_c}(1)}, \frac{1}{\sigma^2_{P_c}(2)}, \cdots, \frac{1}{\sigma^2_{P_c}(n)}\right) \quad (12)$$

Given Eqs. (10) and (12), a weighted least-squares estimate $\hat{\mathbf{C}}$ is used for the estimator of $\mathbf{C}$ and is given by (see [2])

$$\hat{\mathbf{C}} = (\mathbf{A^tRA})^{-1}\mathbf{A^tRY} \quad (13)$$

where the superscript $\mathbf{t}$ is the transpose operator. With $\hat{\mathbf{C}}$ computed and the elements of $\mathbf{C}$ defined in the conscan received signal model, Eq. (8), the cross-elevation and elevation pointing error estimators are chosen as

$$\hat{\varepsilon}_{xel} = \frac{h\hat{\mathbf{C}}_2}{k_s\hat{\mathbf{C}}_1} \quad (14)$$

and

$$\hat{\varepsilon}_{el} = \frac{h\hat{\mathbf{C}}_3}{k_s\hat{\mathbf{C}}_1} \quad (15)$$

The general conscan algorithm also derives the direction of the error $\hat{\varepsilon}_s$ from the relative magnitudes of $\hat{\mathbf{C}}_2$ and $\hat{\mathbf{C}}_3$, together with an operator input phase term, which compensates for time delays in the antenna system. This will not be pursued here, for the present analysis will only focus on the accuracy of the magnitude of the open-loop pointing error estimates.

B. Pointing Error Variance Estimator

In [2] it is shown that the covariance matrix of the error in the estimate $\hat{\mathbf{C}}$ is given by

$$\mathbf{V} = (\mathbf{A^tRA})^{-1} \quad (16)$$

where $\mathbf{A}$ is defined in Eq. (10) and $\mathbf{R}$ by Eq. (12). From Eqs. (14) and (15), the uncertainty in the estimates of $\hat{\varepsilon}_{xel}$ and $\hat{\varepsilon}_{xel}$ must be expressed in terms of the errors of the estimator $\hat{\mathbf{C}}$ (i.e., in terms of 3×3 error covariance $\mathbf{V}$). The calculations are carried out in Appendix A, and the results are presented below:

$$\sigma^2_{\hat{\varepsilon}_{xel}} = \left(\frac{h}{k_s}\right)^2 \left(\frac{1}{P_o}\right)^2 \left[\left(\frac{k_s}{h}\varepsilon_{xel}\right)^2 \mathbf{V}(1,1) + \mathbf{V}(2,2) - 2\left(\frac{k_s}{h}\varepsilon_{xel}\right)\mathbf{V}(1,2)\right] \quad (17)$$

and

$$\sigma^2_{\hat{\varepsilon}_{el}} = \left(\frac{h}{k_s}\right)^2 \left(\frac{1}{P_o}\right)^2 \left[\left(\frac{k_s}{h}\varepsilon_{el}\right)^2 \mathbf{V}(1,1) + \mathbf{V}(3,3) - 2\left(\frac{k_s}{h}\varepsilon_{el}\right)\mathbf{V}(1,3)\right] \quad (18)$$

As can be seen, the axial pointing error variance equations, Eqs. (17) and (18), for conscan are a function of many variables: the average received carrier power P_o, the uncertainties on the carrier power samples (embedded in $\mathbf{V}$), the antenna half-power beamwidth h, the conscan radius r and slope k_s, and the magnitude of the assumed static pointing error ε_s being estimated. Recalling that $\varepsilon_s^2 = \varepsilon_{xel}^2 + \varepsilon_{el}^2$ and $P_o = P_{cnom}L_1L_2$ and noting that the loss factor L_2 appears in both variance equations illustrates the axial cross-coupling of the algorithm (i.e., estimating a large pointing error in one axis will increase the estimation uncertainty in the other). The variance is also a function of the number of input samples (and hence conscan estimation period) that form the measurement distribution matrix $\mathbf{A}$, which in turn influences the covariance matrix $\mathbf{V}$ through Eq. (16). Equations (17) and (18) are, in fact, general for any number of receiver power samples measured uniformly or nonuniformly over the scan.

One important point to note is the dependence of the estimation performance on the operating frequency, which is inversely proportional to the antenna half-power beamwidth h. The radius r can be chosen so that the conscan slope remains constant with respect to operating frequency (e.g., in the DSN, r is typically selected to have a conscan loss of 0.1 dB from the factor L_1 which establishes $k_s = 0.5$ for all frequencies). With k_s constant, the variance can then be seen to be directly proportional to h, or inversely proportional to frequency, indicating a factor of four performance increase at Ka-band (32.0 GHz) over X-band (8.45-GHz) operation. This gain in performance is only realized provided the pointing error ε_s is small, for it will be shown later that loss from the factor L_2 increases dramatically with respect to ε_s at Ka-band.

IV. Analysis of the Conscan Pointing Error Variance Equation

A. Constant Measurement Error Assumption

Now, assuming the uncertainties $\sigma_{P_c(i)}$ on the carrier power samples are constant and equal to σ_{P_c} over the scan period, then the covariance matrix $\mathbf{V}$ defined by Eq. (16) reduces to

$$\mathbf{V} = \sigma_{P_c}^2(\mathbf{A}^t\mathbf{A})^{-1} \tag{19}$$

This is a valid assumption under ideal, closed-loop conscan tracking conditions (benign wind, no spacecraft-induced variations on the downlink signal, etc.) and if the beam-pointing error ε_s is small ($\varepsilon_s \sim r$). Further simplification of $\mathbf{V}$ in Appendix A shows that when the carrier power input is sampled uniformly over the scan period, the pointing error variance Eqs. (17) and (18) each reduce to

$$\sigma_{\hat{\varepsilon}}^2 = \left(\frac{h}{k_s}\right)^2 \left(\frac{1}{n}\right) \left(\frac{\sigma_{P_c}}{P_o}\right)^2 \left(\left(\frac{k_s}{h}\varepsilon\right)^2 + 2\right) \tag{20}$$

where ε represents the actual pointing error in either the elevation or cross-elevation axis.

B. Effects of the Pointing Error Magnitude

1. Performance Degradation Due to Increasing Pointing Errors. Inserting $L_2 = \exp\left((-\mu/h^2)\varepsilon_s^2\right)$ into Eq. (20) and taking the square root gives the axial pointing error standard deviation as

$$\sigma_{\hat{\varepsilon}} = \left(\frac{h}{k_s}\right) \left(\frac{1}{n}\right)^{\frac{1}{2}} \left(\frac{\sigma_{P_c}}{P_{cnom}L_1}\right) \left(\frac{1}{\exp(-\frac{\mu}{h^2}\varepsilon_s^2)}\right) \times \left(\left(\frac{k_s}{h}\varepsilon\right)^2 + 2\right)^{\frac{1}{2}} \tag{21}$$

where ε_s is the beam-pointing error and ε is the axial-pointing error. By simple inspection, the last factor can be accurately approximated by

$$\left(\left(\frac{k_s}{h}\varepsilon\right)^2 + 2\right)^{\frac{1}{2}} \sim \sqrt{2} \tag{22}$$

when $\varepsilon \leq h$ and the conscan slope is chosen as $k_s = 0.5$ for the DSN application. For reference, the half-power beamwidths (assuming a Gaussian beam) for a 34-m antenna operating at the X- and Ka-band frequencies are approximately 65 and 17 mdeg, respectively. Thus, as the magnitude of the beam-pointing error $\varepsilon_s = (\varepsilon_{xel}^2 + \varepsilon_{el}^2)^{1/2}$ increases, both estimates $\hat{\varepsilon}_{xel}$ and $\hat{\varepsilon}_{xel}$ are degraded equally by the inverse of the pointing-error loss factor $\exp\left((-\mu/h^2)\varepsilon_s^2\right)$. This effect is obviously more dramatic at Ka-band due to the narrow beamwidth. Figure 1 illustrates the percentage of increase of the axial pointing error standard deviation $\hat{\varepsilon}$ against the magnitude of ε_s for a 34-m antenna operating at the X- and Ka-band frequencies. In addition to dropping received carrier power by 3 dB at Ka-band, a beam-pointing error of 8.5 mdeg (one-half of the full half-power beamwidth h) is seen in Fig. 1 to double the Ka-band conscan estimation uncertainty. Without considering actual receiver signal-to-noise operating conditions, this Ka-band performance degradation will primarily affect conscan during acquisition, when blind pointing errors may be large. For the closed-loop system, this degradation will effectively increase the beam-pointing error response time.

2. Zero Pointing Error Assumption. As noted before, the magnitude of beam-pointing error ε_s is typically very small during closed-loop conscan tracking. This fact can be used to further simplify Eq. (21) in order to quantify the performance of the conscan pointing error estimator as a function of the carrier power-to-uncertainty ratio and the selectable input variables. Assuming ε_s is essentially zero, then Eq. (21) reduces to

$$\sigma_{\hat{\varepsilon}} = \left(\frac{h}{k_s}\right) \left(\frac{2}{n}\right)^{\frac{1}{2}} \left(\frac{1}{L_1}\right) \left(\frac{P_{cnom}}{\sigma_{P_c}}\right)^{-1} \tag{23}$$

where it is recalled that P_{cnom} is the nominal carrier power received when the antenna is pointing directly at the target and the uncertainty σ_{P_c} is assumed to be known.

V. Carrier Power Uncertainty for the Block V Receiver Subsystem

Estimation of the uncertainties $\sigma_{P_c}(i)$ on the carrier power samples $P_c(i)$ in the Block V Receiver Subsystem is briefly summarized in Appendix B. In general, calculation and analysis of this statistic for spacecraft tracking in a DSN antenna environment is a complicated matter. For this reason, it will not be rigorously pursued here; for a more thorough analysis, the details of the Block V receiver calculation can be found in [3,4], Aung, et al.,[1] and Scheid.[2] Of more interest in the present analysis is the approximation of the expression for σ_{P_c} given in the references, so that Eq. (23) can be written in terms of the nominal receiver carrier-to-noise power ratio $CNR = P_{cnom}/N_o$ instead of P_{cnom}/σ_{P_c}. The quantity CNR is measured when the antenna is pointed directly at the spacecraft. The simplification is carried out in Appendix B with the following result

$$\sigma_{P_c} \approx (2P_{cnom}N_o)^{\frac{1}{2}} \qquad (24)$$

which is a valid approximation for a 1-sec receiver estimation period when the loop tracking error is very small and $P_{cnom}/N_o < 40$ dB-Hz. Now, inserting this expression into the conscan pointing-error estimation Eq. (23) and simplifying yields

$$\sigma_{\hat{\epsilon}} = \left(\frac{h}{k_s}\right)\left(\frac{1}{n}\right)^{\frac{1}{2}}\left(\frac{2}{L_1}\right)(CNR^{-1})^{\frac{1}{2}} \qquad (25)$$

Equation (25) is a very useful equation as it allows quick evaluation of the pointing error estimation accuracy as a function of the selectable conscan algorithm input (radius r and number of input samples n) for any given operating CNR and antenna half-power beamwidth h.

[1] M. Aung and S. Stephens, "Statistics of the P_c/N_o Estimator in the Block V Receiver," JPL Interoffice Memorandum 3338-92-089 (internal document), Jet Propulsion Laboratory, Pasadena, California, April 29, 1992.

[2] R. E. Scheid, "Statistical Analysis of Antenna Carrier Power," JPL Interoffice Memorandum 343-92-1291 (internal document), Jet Propulsion Laboratory, Pasadena, California, October 9, 1992.

VI. Application to a 34-m Antenna Beam-Waveguide Mirror Conscan System at Ka-Band

All of the conscan equations thus far have been general, but they will now be applied to a 34-m beam-waveguide mirror-based conscan system operating at Ka-band. For this scenario, $h = 17$ mdeg and the radius $r = 1.55$ mdeg for a scan loss of 0.1 dB ($L_1 = 0.977$) and $k_s = 0.5$. These values are inserted into Eq. (25), and the axial pointing error standard deviation $\sigma_{\hat{\epsilon}}$ is then plotted in Fig. 2 as a function of conscan period for various CNR. Also plotted is the line corresponding to the magnitude of the chosen radius r. In Fig. 2, it is assumed that the receiver integration time per carrier power sample is 1 sec and the conscan period is then just equal to n. This performance plot implies that for $CNR \geq 30$ dB-Hz, the conscan estimation period for Ka-band operation may be chosen well below the current DSN minimum of 32 sec and still maintain estimation accuracy of less than 1.55 mdeg.

Advantages of scanning a beam-waveguide mirror instead of the entire antenna dish structure include the ease of obtaining precision pointing of a drastically smaller and stiffer mirror gimbal assembly and also the higher bandwidths achievable by the small-scale axis servos. A conceptual sketch of such a system is presented in Fig. 3, in which it is proposed that either the first or last beam waveguide mirror be actuated in such a conscan scheme. Because high-rate, accurate mirror tracking is available, it was assumed in the previous Ka-band performance plot that the move times between measurement points over the scan are negligible. In fact, with an efficient interface between the conscan computer and the receiver subsystem, it is conceivable that the mirror-based conscan system can actually achieve pointing correction update rates as ambitious as those shown in Fig. 2.

VII. Summary and Future Work

General pointing error and variance estimators for conscan have been derived in order to characterize the estimated performance in terms of the operator-selectable input to the algorithm and carrier-to-noise ratio. After assuming constant measurement noise on the carrier power inputs in the variance equation, it was shown that the magnitude of the beam-pointing error being estimated degrades performance in each axis of the estimator. The effect is especially dramatic when conscaning at the Ka-band frequency due to the the narrow antenna half-power beamwidths. For the closed-loop conscan tracking application, the zero pointing error assumption was applied in order to express the pointing error estimation accuracy as a function of the selectable algorithm input (radius and number of input samples) for any given operating carrier power to the uncertainty ratio and antenna half-power beamwidth. The performance equation was then applied to a 34-m beam-waveguide, mirror-based conscan system interfaced with the Block V Receiver Subsystem tracking a Ka-band downlink. Simulation of conscan pointing error uncertainty against conscan estimation period showed that for a carrier-to-noise power $\geq$ 30 dB-Hz, the period for Ka-band operation may be chosen well below the current DSN minimum of 32 sec and still maintain estimation accuracy of less than 1.55 mdeg.

The analysis presented forms the basis of future conscan work in both research and development as well as for the upcoming DSN antenna controller upgrade for the new DSS-24, 34-m beam-waveguide antenna. The conscan model and performance equations derived will be used in designing advanced tracking algorithms and generating predictions for experimentation on the new beam-waveguide mirror conscan system currently being implemented at the DSS-13 antenna. These equations will also be utilized in the DSN conscan upgrade, which will use an automatic algorithm parameter selection as a function of signal-to-noise input ratio. Lastly, an augmented analysis that integrates the effects of spacecraft spin (as in [5]) and dynamic wind loading on the antenna structure needs to be pursued in order to more precisely simulate open- and closed-loop conscan performance at the Ka-band frequency.

Acknowledgment

The author wishes to thank Mike Thorburn for his helpful technical discussions and encouragement.

References

[1] G. Biernson, *Optimal Radar Tracking Systems*, New York, New York: John Wiley and Sons, Inc., 1990.

[2] A. E. Bryson and Y. Ho, *Applied Optimal Control*, Waltham, Massachusetts: Blaisdell Publishing Company, 1969.

[3] A. M. Monk, "Carrier-to-Noise Power Estimation for the Block V Receiver," *The Telecommunications and Data Acquisition Progress Report 42-106, vol. April–June 1991*, Jet Propulsion Laboratory, Pasadena, California, pp. 353–363, August 15, 1991.

[4] T. J. Brunzie, "The Parkes Front-End Controller and Noise-Adding Radiometer," *The Telecommunications and Data Acquisition Progress Report 42-102, vol. April–June 1990*, Jet Propulsion Laboratory, Pasadena, California, pp. 119–137, August 15, 1990.

[5] A. Mileant, and T. Peng, "Pointing a Ground Antenna at a Spinning Spacecraft Using Conscan-Simulation Results," *The Telecommunications and Data Acquisition Progress Report 42-95, vol. July–September 1988*, Jet Propulsion Laboratory, Pasadena, California, pp. 246–260, November 15, 1988.

Appendix A
Simplification of the Conscan Pointing Error Estimation Variance

Assuming that the uncertainties $\sigma_{P_c}(i)$ on the ith carrier power sample are random and independent, then the covariance matrix of the error in the weighted least squares estimator $\hat{\mathbf{C}}$ of Eq. (13) is given by

$$\mathbf{V} = (\mathbf{A}^t\mathbf{R}\mathbf{A})^{-1} \tag{A-1}$$

where the measurement distribution matrix $\mathbf{A}$ is

$$\mathbf{A} = \begin{bmatrix} 1 & \cos(\frac{2\pi}{n}) & \sin(\frac{2\pi}{n}) \\ 1 & \cos(2\frac{2\pi}{n}) & \sin(2\frac{2\pi}{n}) \\ & \vdots & \\ 1 & \cos(2\pi) & \sin(2\pi) \end{bmatrix} \tag{A-2}$$

and the weighting matrix $\mathbf{R}$ is

$$\mathbf{R} = \mathrm{diag}\left(\frac{1}{\sigma^2_{P_c}(1)}, \frac{1}{\sigma^2_{P_c}(2)}, \cdots, \frac{1}{\sigma^2_{P_c}(n)}\right) \tag{A-3}$$

Given the above expressions, Eq. (A-1) can be expanded as follows

$$\mathbf{V} = \begin{bmatrix} \sum \frac{1}{\sigma^2_{P_c(i)}} & \sum \frac{1}{\sigma^2_{P_c(i)}} \cos(\frac{2\pi}{n} i) & \sum \frac{1}{\sigma^2_{P_c(i)}} \sin(\frac{2\pi}{n} i) \\ \sum \frac{1}{\sigma^2_{P_c(i)}} \cos(\frac{2\pi}{n} i) & \sum \frac{1}{\sigma^2_{P_c(i)}} \cos^2(\frac{2\pi}{n} i) & \sum \frac{1}{\sigma^2_{P_c(i)}} \cos(\frac{2\pi}{n} i)\sin(\frac{2\pi}{n} i) \\ \sum \frac{1}{\sigma^2_{P_c(i)}} \sin(\frac{2\pi}{n} i) & \sum \frac{1}{\sigma^2_{P_c(i)}} \cos(\frac{2\pi}{n} i)\sin(\frac{2\pi}{n} i) & \sum \frac{1}{\sigma^2_{P_c(i)}} \sin^2(\frac{2\pi}{n} i) \end{bmatrix}^{-1} \tag{A-4}$$

where the summations run over $i = 1, 2, \cdots, n$, and n is the total number of samples taken over the scan. If the measurement uncertainties are assumed to be constant over this period and equal to σ_{P_c}, then Eq. (A-4) simplifies to

$$\mathbf{V} = \sigma^2_{P_c} \begin{bmatrix} n & \sum \cos(\frac{2\pi}{n} i) & \sum \sin(\frac{2\pi}{n} i) \\ \sum \cos(\frac{2\pi}{n} i) & \sum \cos^2(\frac{2\pi}{n} i) & \sum \cos(\frac{2\pi}{n} i)\sin(\frac{2\pi}{n} i) \\ \sum \sin(\frac{2\pi}{n} i) & \sum \cos(\frac{2\pi}{n} i)\sin(\frac{2\pi}{n} i) & \sum \sin^2(\frac{2\pi}{n} i) \end{bmatrix}^{-1} \tag{A-5}$$

Now if the samples $P_c(i)$ are measured uniformly over the scan period as indicated above and $n \geq 3$, then Eq. (A-5) simplifies to

$$\mathbf{V} = \sigma^2_{P_c} \begin{bmatrix} \frac{1}{n} & 0 & 0 \\ 0 & \frac{2}{n} & 0 \\ 0 & 0 & \frac{2}{n} \end{bmatrix} \tag{A-6}$$

The conscan pointing-error estimation variances are derived from the following pointing-error estimator equations

$$\hat{\varepsilon}_{xel} = \frac{h\hat{\mathbf{C}}_2}{k_s\hat{\mathbf{C}}_1} \tag{A-7}$$

$$\hat{\varepsilon}_{el} = \frac{h\hat{\mathbf{C}}_3}{k_s\hat{\mathbf{C}}_1} \tag{A-8}$$

To find the variances of these estimates (each of which is a function of two random variables from $\hat{\mathbf{C}}$), the following formula is applied:

$$VAR(\hat{\varepsilon}) = \left(\frac{\partial\hat{\varepsilon}}{\partial\hat{\mathbf{C}}_1}\right)^2 VAR(\hat{\mathbf{C}}_1) + \left(\frac{\partial\hat{\varepsilon}}{\partial\hat{\mathbf{C}}_j}\right)^2 VAR(\hat{\mathbf{C}}_j) + 2\frac{\partial\hat{\varepsilon}}{\partial\hat{\mathbf{C}}_1}\frac{\partial\hat{\varepsilon}}{\partial\hat{\mathbf{C}}_j} VAR(\hat{\mathbf{C}}_1, \hat{\mathbf{C}}_j) \tag{A-9}$$

for $j = 2, 3$ and where the partial derivatives are evaluated at the statistical averages of the estimators $\hat{\mathbf{C}}_i, i = 1, 2, 3$. It can easily be proved that the statistical average of $\hat{\mathbf{C}}$ is just the vector $\mathbf{C}$, whose elements are defined by the conscan received signal model given in Eq. (8). Thus, the partial derivatives above are to be evaluated at $\mathbf{C}_1 = P_o$, $\mathbf{C}_2 = ((k_s/h)\varepsilon_{xel})\,P_o$, and $\mathbf{C}_3 = ((k_s/h)\varepsilon_{xel})\,P_o$. Applying the formula in Eq. (A-9) to Eqs. (A-7) and (A-8) yields

$$\sigma^2_{\hat{\varepsilon}_{xel}} = \left(\frac{h}{k_s}\right)^2 \left(\frac{\mathbf{C}_2^2}{\mathbf{C}_1^4}\mathbf{V}(1,1) + \frac{1}{\mathbf{C}_1^2}\mathbf{V}(2,2) - 2\frac{\mathbf{C}_2}{\mathbf{C}_1^3}\mathbf{V}(1,2)\right) \tag{A-10}$$

and

$$\sigma^2_{\hat{\varepsilon}_{el}} = \left(\frac{h}{k_s}\right)^2 \left(\frac{\mathbf{C}_3^2}{\mathbf{C}_1^4}\mathbf{V}(1,1) + \frac{1}{\mathbf{C}_1^2}\mathbf{V}(3,3) - 2\frac{\mathbf{C}_3}{\mathbf{C}_1^3}\mathbf{V}(1,3)\right) \tag{A-11}$$

Next, inserting the given expressions for the elements of $\mathbf{C}$ and using $\mathbf{V}$ defined by Eq. (A-6) for the constant measurement error case, the above variance equations can be rewritten as

$$\sigma^2_{\hat{\varepsilon}_{xel}} = \left(\frac{h}{k_s}\right)^2 \left(\left(\frac{k_s}{hP_o}\varepsilon_{xel}\right)^2 \frac{\sigma^2_{P_c}}{n} + \frac{2\sigma^2_{P_c}}{nP_o^2}\right) \tag{A-12}$$

and

$$\sigma^2_{\hat{\varepsilon}_{el}} = \left(\frac{h}{k_s}\right)^2 \left(\left(\frac{k_s}{hP_o}\varepsilon_{el}\right)^2 \frac{\sigma^2_{P_c}}{n} + \frac{2\sigma^2_{P_c}}{nP_o^2}\right) \tag{A-13}$$

Finally, after some rearranging, Eqs. (A-12) and (A-13) can be rewritten as

$$\sigma^2_{\hat{\varepsilon}} = \left(\frac{h}{k_s}\right)^2 \left(\frac{1}{n}\right) \left(\frac{\sigma_{P_c}}{P_o}\right)^2 \left(\left(\frac{k_s}{h}\varepsilon\right)^2 + 2\right) \tag{A-14}$$

where ε represents the actual pointing error in either the elevation or cross-elevation axis.

Appendix B

Received Carrier Power Uncertainty for the Block V Receiver

Inputs to the conical scan algorithm are estimates of received carrier power P_c and its uncertainty σ_{P_c}. A brief summary of the Block V receiver variance estimator is given below; however, a more detailed derivation may be obtained from [3] and footnotes 1 and 2. The receiver calculates σ_{P_c} from its estimates of signal-to-noise ratio (P_c/N_o) and variance $\sigma^2_{(P_c/N_o)}$, and system noise power N_o and variance $\sigma^2_{N_o}$. The system noise power over a 1-Hz bandwidth is $N_o = \kappa T_{sys}$, where T_{sys} is the system noise temperature with standard deviation $\sigma_{T_{sys}}$ (defined in [4]) and κ is Boltzmann Constant. The estimated noise power variance is then given by $\sigma^2_{N_o} = \kappa^2\sigma^2_{T_{sys}}$. Multiplication negates the noise power from the received carrier signal power as follows:

$$P_c = \left(\frac{P_c}{N_o}\right) N_o \tag{B-1}$$

Now, assuming that the above equation is the product of two independent random variables, the carrier power variance can then be shown to be

$$\sigma^2_{P_c} = \sigma^2_{N_o}\left(\overline{\frac{P_c}{N_o}}\right)^2 + \sigma^2_{\left(\frac{P_c}{N_o}\right)}\overline{N}_o^{\,2} + \sigma^2_{N_o}\sigma^2_{\left(\frac{P_c}{N_o}\right)} \tag{B-2}$$

where the overbar denotes average values. Equation (B-2) gives the uncertainty of the received carrier power P_c in terms of the uncertainties of the estimates of (P_c/N_o) and (N_o). As described in [3] and footnote 1, the statistics of (P_c/N_o) are a function of receiver parameters (i.e., P_c/N_o, tracking loop error, tracking loop bandwidth, estimation interval, etc.) while the statistics of N_o are given as a function of T_{sys}, noise diode temperature, noise bandwidth, and estimation interval.

For this article, it is best to express the uncertainty on the carrier power in terms of the receiver carrier power P_c and the system noise power N_o. In [3], in-phase arm (I-arm) and in-phase/quadrature-phase arm (IQ-arm) P_c/N_o algorithms are presented. Of the two, a slightly modified version of the I-arm estimator will be implemented in the Block V receiver (see footnote 1). The equation for the variance of this estimator given in footnote 1 can be approximated by

$$\sigma^2_{\left(\frac{P_c}{N_o}\right)} \approx 2\left(\overline{\frac{P_c}{N_o}}\right) \tag{B-3}$$

assuming a 1-sec receiver estimation period when the loop tracking error ϕ is small enough so that $\cos(\phi) \approx 1$. Numerical simulation of Eq. (B-2) shows that for $P_c/N_o < 40$ db-Hz the contribution of the noise power variance σ_{N_o} in the calculation of σ_{P_c} is minimal and can be neglected. From Eq. (B-3), the carrier power uncertainty can then be reduced to

$$\sigma_{P_c} \approx \sigma_{\left(\frac{P_c}{N_o}\right)}\overline{N}_o \tag{B-4}$$

or inserting $\sigma_{(P_c/N_o)}$ from Eq. (B-3) and simplifying yields

$$\sigma_{P_c} \approx \left(2\overline{P}_c\overline{N}_o\right)^{\frac{1}{2}} \tag{B-5}$$

which is the desired approximation.

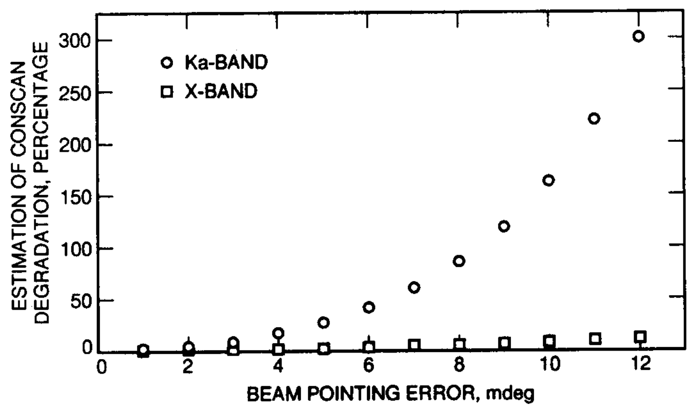

Fig. 1. Conscan estimation performance degradation due to increasing pointing error for a 34-m antenna.

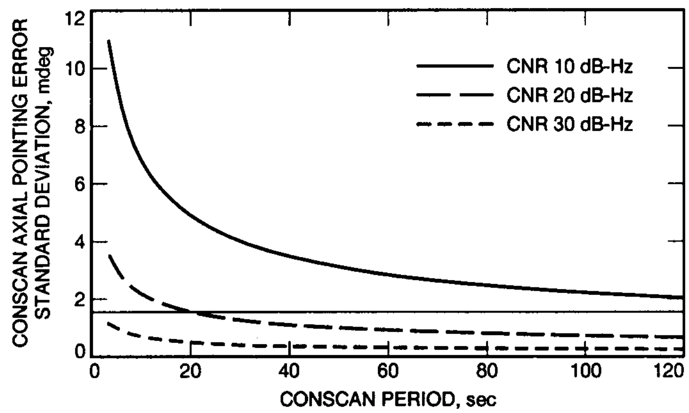

Fig. 2. Open-loop conscan axial pointing-error estimation accuracy for a 34-m antenna operating at Ka-band.

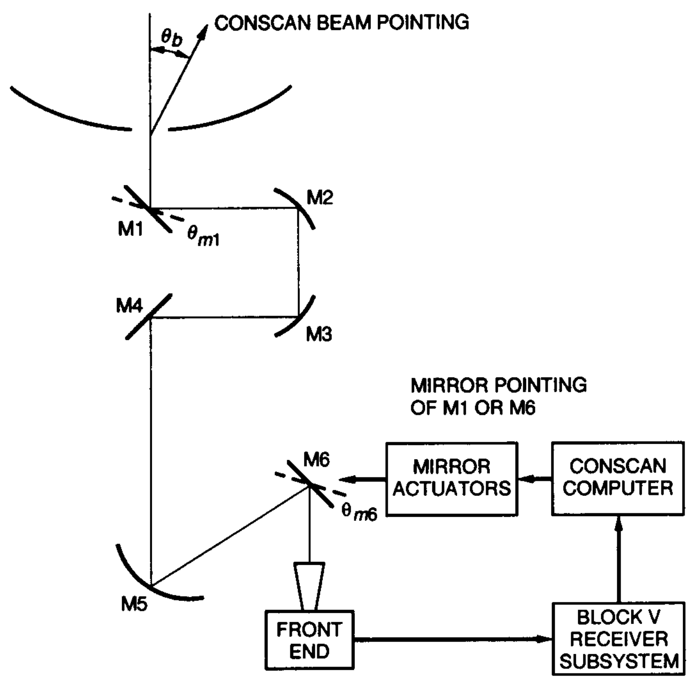

Fig. 3. Conceptual diagram of a 34-m beam-waveguide antenna mirror-based conscan system.